Journal of Solid Mechanics Vol. 5, No. 2 (2013) pp. 174-192

Design and Dynamic Modeling of Planar Parallel Micro-Positioning Platform Mechanism with Flexible Links Based on Euler Bernoulli Beam Theory

N.S. Viliani[1,*], H. Zohoor[2], M.H. Kargarnovin[3]

[1]*Department of Mechanical and Aerospace Engineering, Science and Research Branch, Islamic Azad University, Tehran, Iran*
[2]*Center of Excellence in Design, Robotics, and Automation, Sharif University of Technology; Fellow, The Academy of Sciences of Iran, Tehran, Iran*
[3]*School of Mechanical Engineering, Sharif University of Technology, Tehran, Iran*

Received 24 March 2013; accepted 16 May 2013

ABSTRACT

This paper presents the dynamic modeling and design of micro motion compliant parallel mechanism with flexible intermediate links and rigid moving platform. Modeling of mechanism is described with closed kinematic loops and the dynamic equations are derived using Lagrange multipliers and Kane's methods. Euler-Bernoulli beam theory is considered for modeling the intermediate flexible link. Based on the Assumed Mode Method theory, the governing differential equations of motion are derived and solved using both Runge-Kutta-Fehlberg4, 5th and Perturbation methods. The mode shapes and natural frequencies are calculated under clamped-clamped boundary conditions. Comparing perturbation method with Runge-Kutta-Fehlberg4, 5th leads to same results. The mode frequency and the effects of geometry of flexure hinges on intermediate links vibration are investigated and the mode frequency, calculated using Fast Fourier Transform and the results are discussed.

Keywords: Compliant mechanism; Flexible link; Kane's method; Micro positioning; Lagrange multipliers

1 INTRODUCTION

COMPLIANT mechanism with parallel structures that provide the required motion by flexure hinges, have been adopted in many small-scale applications. In order to use flexure hinges, compliant mechanism makes smooth motions without problems such as friction losses, need for lubrication, hysteresis, maintenance, and drawbacks. Clearly, precision is the most important factor for micro positioning applications[21].

For this purpose, the flexibility of link improves accuracy and some other characteristics of manipulator such as minimizing the energy needed to run the manipulator, increasing speed, and reducing the internal stresses and displacement [24, 26, and 27]. In the case of flexible manipulators, Zhou et al. [28] established dynamic equations of flexible (3PRS) manipulator for vibration analysis using the finite element method (FEM).A dynamic model was developed based on FEM for a 3-PRR planar parallel manipulator with flexible links in reported works [29, 30].

The basis work of the flexure hinges was presented by Paros and Weisbord [6]. In kinematic and dynamic modeling of compliant mechanisms, the Pseudo-Rigid-Body Model (PRBM) approach is the almost unique method that is used in most of researches. The PRBM is used to predict the displacement of compliant mechanism and

* Corresponding author. Tel.: +98 21 2237 8012.
E-mail address: Navid.Viliani@gmail.com (N. Viliani).

models the flexure hinge as a revolute joint with an attached torsional spring. Considerable results from applying this concept to compliant mechanisms have been obtained by Anathasuresh and Kota [7], Murphy et al. [8]; Saggere and Kota [10]; Yu et al. [20]; and Kota et al. [11]. However, the flexure hinge has also translational motion although the amount of axial deformation of flexure hinges is small [2].The accuracy of Pseudo-Rigid-Body Model is reduced when the x and y deformation of flexure hinges are ignored [3, 5].

Most of the previous studies modeled the flexure hinge by using 1DOF for a revolute hinge. However, the flexure hinge has also translational motion even though the amount is small [2].The accuracy of the kinematics predicted using PRBM is reduced when the x and y deformation of flexure hinges are ignored [3].

Flexure hinges have different profiles [1], but circular hinges have been widely used in compliant mechanism. Paros and Weisbord [6] and Rong et al. [12] derived analytical compliance equations of circular flexure hinges. Her and Cheng [13] used finite element approach to numerically determine the rotational stiffness of circular flexure hinges and developed a linear scheme for displacement analysis of compliant mechanism based on the PRBM method and linearization of the geometric constraint equations of a compliant structure. Lobontiu et al. [16] derived analytical equations to predict the compliances of the corner-filleted flexure hinges along all three axes. They used Castiglione's second theorem to derive the compliance equations and they found that corner-filleted hinges could deform more but induce lower stresses than that of circular hinges.

Shim et al. [17] derived a kinematic model of a six-DOF micro-positioning parallel. The model was derived using the PRBM method. However, they did not compare the analytical model with FEA simulations or experimental results. Ryu et al. [18] developed a XYθ compliant mechanism with three piezo-actuators. Zhang et al. developed a 3-RRR compliant stage. A kinematic model of the stage was derived base on PRBM and x and y deformation of flexure hinges was not considered in the model. Yong et al. [3, 4, and 5] presented the kinetostatic model of a flexure-based 3-RRR compliant micro-motion stage and investigated the effect of the accuracies of flexure hinge equations. Two cases were studied where two kinetostatic results were obtained using two different sets of flexure hinge equations and then kinetostatic results were compared to the finite-element-analysis results to verify their accuracies.

Y. Tian et al. [22] developed the in-plane and out-of-plane stiffnesses of the flexure hinges derived and the influences of the geometric parameters on the performance of the flexure hinges are investigated. In this paper dynamic analysis of a compliant micro-motion stage mechanism with three flexible intermediate links is presented. This mechanism has $3+3r$ degrees of freedom. The 3RPR links arranged in parallel and each link has 2 circular flexure hinges. Each intermediate link has been treated as a Euler-Bernoulli beam. Structural dynamic equations of the proposed compliant mechanism are derived based on Lagrange multiplier and Kane's methods. Also the AMM is adopted to discretize the distributed dynamic system of the manipulator system with flexible links and solved using Perturbation method and results for the deflection of the intermediate link is compared with Runge-Kutta-Fehlberg 4,5th. Further, numerical simulations are performed and the assumed mode shapes and frequencies of links to be obtained based on clamped-clamped boundary conditions. The natural frequency for each assumed mode and the effects of hinges length on vibration of links are investigated.

Fig. 1
Modeling of parallel micro-positioning compliant mechanism.

2 COMPLIANT MICRO-MOTION SYSTEM CONFIGURATION

The present parallel compliant mechanism consists of three chains that connect the end-effector to a fixed base. The three chains are 120 degree apart from each other and mechanism also has a symmetrical configuration. The compliant micro-motion mechanism illustrated in Fig. 1. The end- effector translates along x and y axis and rotates about the z axis. The first flexure hinge in each chain is modeled as having 2DOF hinge. Consequently, first hinge

assumes that the flexure hinges in the mechanism act like a 1DOF revolute joint and a 1DOF prismatic joint and the second flexure hinges in each chain is modeled as a revolute joint. The shape of the circular flexure hinge is depicted in Fig. 2.

In order to facilitate the formulation of kinematics and dynamics, all coordinates and loops are shown in Fig. 3. The three chains are 120 degree apart from each other and mechanism also has a symmetrical configuration, and thus is less sensitive to temperature gradient that could change the kinematics of structure due to material expansion or contraction. The B_iC_i are assumed flexible. The first revolute joint in each of chains is active joint and other ones are passive joint.

(a) (b)

Fig. 2
Schematic of the flexure hinge (a): Real model, (b): Mechanical model.

3 KINEMATIC MODEL

Loop-closure theory incorporates the complex number method to model a mechanism.

From the loop1,

$$\overline{A_2B_2}+\overline{u}_2+\overline{L_2}+\overline{C_1C_2}=\overline{A_2A_1}+\overline{A_1B_1}+\overline{u_1}+\overline{L_1} \tag{1}$$

From loop2,

$$\overline{A_2B_2}+\overline{u}_2+\overline{L_2}+\overline{C_2C_3}=\overline{A_2A_3}+\overline{A_3B_3}+\overline{u_3}+\overline{L_3} \tag{2}$$

where L_1, L_2, L_3 are the length of links and $u_i(t)$ are axial deformation of flexure hinges. Since the angular displacements of the compliant mechanism are small, the small angle approximation of cosine and sine functions can be adopted, which $\sin(\beta_i)=\beta_i$, $\cos(\beta_i)=1$. By using real and imaginary component and trigonometric identity and some mathematical manipulation of the Eqs.1 and 2 can be simplified as:

$$\begin{aligned} &l_{flex}\cos(\alpha_2)-l_{flex}\sin(\alpha_2)\beta_2+u_2\cos(\alpha_2)-u_2\sin(\alpha_2)\beta_2+u_3\sin(\alpha_3)\beta_3-u_2\sin(\alpha_2)\beta_2+\\ &L_2\cos(\alpha_2)-L_2\sin(\alpha_2)\beta_2+C_2C_3\cos(\alpha_{c_2c_3})-C_2C_3\cos(\alpha_{c_2c_3})\beta_2\alpha_{c_2}-C_2C_3\sin(\alpha_{c_2c_3})\beta_2-\\ &C_2C_3\sin(\alpha_{c_2c_3})\alpha_{c_2}-A_2A_3\cos(\alpha_{A_2A_3})-l_{flex}\cos(\alpha_3)+l_{flex}\sin(\alpha_3)\beta_3-u_3\cos(\alpha_3)+u_3\sin(\alpha_3)\beta_3\\ &-L_3\cos(\alpha_3)+L_3\sin(\alpha_3)\beta_3=0 \end{aligned} \tag{3a}$$

and $l_{flex}\cos(\alpha_2)+L_2\cos(\alpha_2)+C_2C_3\cos(\alpha_{C_2C_3})-l_{flex}\cos(\alpha_3)-L_3\cos(\alpha_3)=A_2A_3\cos(\alpha_{A_2A_3})$, therefore Eq.(3a) can be reduced to:

$$\begin{aligned} &u_3\sin(\alpha_3)\beta_3-u_2\sin(\alpha_2)\beta_2+(-\sin(\alpha_2)\beta_2+\sin(\alpha_3)\beta_3)l_{flex}-L_2\sin(\alpha_2)\beta_2+L_3\sin(\alpha_3)\beta_3\\ &+(-\sin(\alpha_{C_2C_3})\beta_2-\sin(\alpha_{C_2C_3})\alpha_{c_2})C_2C_3+u_2\cos(\alpha_2)-u_3\cos(\alpha_3)+C_2C_3\cos(\alpha_{C_2C_3})\beta_2\alpha_{C_2}=0 \end{aligned} \tag{3b}$$

Loop equation obtained from the imaginary component of Eq. 2 is:

$$
\begin{aligned}
&l_{flex}\sin(\alpha_2)+l_{flex}\cos(\alpha_2)\beta_2+u_2\sin(\alpha_2)+u_2\cos(\alpha_2)\beta_2+u_3\cos(\alpha_3)\beta_3+\\
&u_2\cos(\alpha_2)\beta_2+L_2\sin(\alpha_2)+L_2\cos(\alpha_2)\beta_2+C_2C_3\sin(\alpha_{c_2c_3})-\\
&C_2C_3\sin(\alpha_{c_2c_3})\beta_2\alpha_{c_2}+C_2C_3\cos(\alpha_{C_2C_3})\beta_2+C_2C_3\cos(\alpha_{C_2C_3})\alpha_{c_2}-\\
&A_2A_3\sin(\alpha_{A_2A_3})-l_{flex}\sin(\alpha_3)-l_{flex}\cos(\alpha_3)\beta_3-u_3\sin(\alpha_3)-u_3\cos(\alpha_3)\beta_3\\
&-L_3\sin(\alpha_3)-L_3\cos(\alpha_3)\beta_3=0
\end{aligned}
\tag{4a}
$$

and $l_{flex}\sin(\alpha_2)+L_2\sin(\alpha_2)+C_2C_3\sin(\alpha_{C_2C_3})-l_{flex}\sin(\alpha_3)-L_3\sin(\alpha_3)=A_2A_3\sin(\alpha_{A_2A_3})$ therefore Eq.(4a) can be reduced to:

$$
\begin{aligned}
&-u_3\cos(\alpha_3)\beta_3+u_2\cos(\alpha_2)\beta_2+(\cos(\alpha_2)\beta_2-\cos(\alpha_3)\beta_3)l_{flex}+L_2\cos(\alpha_2)\beta_2-L_3\cos(\alpha_3)\beta_3+\\
&(\cos(\alpha_{C_2C_3})\beta_2+\cos(\alpha_{C_2C_3})\alpha_{C_2})C_2C_3-C_2C_3\sin(\alpha_{C_2C_3})\beta_2\alpha_{C_2}+u_2\sin(\alpha_2)-u_3\sin(\alpha_3)=0
\end{aligned}
\tag{4b}
$$

According to the above simplification Eq. (1) can be obtained:

$$
\begin{aligned}
&u_1\sin(\alpha_1)\beta_1-u_2\sin(\alpha_2)\beta_2+(-\sin(\alpha_2)\beta_2+\sin(\alpha_1)\beta_1)l_{flex}-L_2\sin(\alpha_2)\beta_2+L_1\sin(\alpha_1)\beta_1\\
&+(-\sin(\alpha_{C_1C_2})\beta_2-\sin(\alpha_{C_1C_2})\alpha_{c_2})C_1C_2+u_2\cos(\alpha_2)-u_1\cos(\alpha_1)+C_1C_2\cos(\alpha_{C_1C_2})\beta_2\alpha_{C_2}=0
\end{aligned}
\tag{5}
$$

$$
\begin{aligned}
&-u_1\cos(\alpha_1)\beta_1+u_2\cos(\alpha_2)\beta_2+(\cos(\alpha_2)\beta_2-\cos(\alpha_1)\beta_1)l_{flex}+L_2\cos(\alpha_2)\beta_2-L_1\cos(\alpha_1)\beta_1\\
&+(\cos(\alpha_{C_1C_2})\beta_2+\cos(\alpha_{C_1C_2})\alpha_{c_2})C_1C_2+u_2\sin(\alpha_2)-u_1\sin(\alpha_1)-C_1C_2\sin(\alpha_{C_1C_2})\beta_2\alpha_{C_2}=0
\end{aligned}
\tag{6}
$$

In which $\alpha_{C_1C_2}$, $\alpha_{C_2C_3}$ and $\alpha_{A_2A_3}$ are arguments of vector $\overline{C_1C_2}$, $\overline{C_2C_3}$ and $\overline{A_2A_3}$ measured in the global X-axis and l_{flex} is the length of the first flexure hinges in each chain. In the above equations α_{C_2} and u_i, $i=1,2,3$ are unknowns. Therefore, there are only four unknowns which required only four equations. For the compliant mechanism, there are three inputs that are given as the function of three input rotations. These are in turn by turning a function of the PZT displacements, $l_{1pzt}, l_{2pzt}, l_{3pzt}$ respectively. The three inputs are:

$$
\beta_i=\frac{l_{ipzt}}{d}
\tag{7}
$$

where d is distance from A_i to the center of piezo-actuator and l_{ipzt} is input displacement by the pizo-actuator. Table 1.exhibit all parameters of compliant mechanism.

Fig. 3
Coordinate system of the 3-RPR parallel compliant mechanism.

4 DYNAMIC MODELING

Lagrange multipliers and Kane's method adopted to derive dynamic equation of motion of parallel the compliant mechanism with three flexible intermediate links. For the Lagrange method the total kinetic and potential energy are evaluated and for the Kane's method quasi velocities and acceleration of the center of mass for each flexible link must be evaluated.

4.1 Kinetic and potential energy of ith links

In this paper, for the intermediate flexible links, the dynamic equations of parallel compliant mechanism are developed using Euler-Bernoulli beam theory. One of the links as shown in Fig. 4. The component $W_i(x,t)$ represents the transverse displacement of link i^{th} link at a distance x from the joint coordinate system along the x axis. $\alpha_i + \beta_i(t)$ represents the angle between the link and the horizontal axis and $u_i(t)$ are axial deformation of flexure hinges.

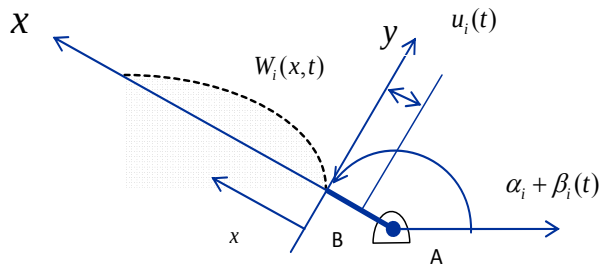

Fig. 4
Compliant mechanism with flexure hinge and flexible link

The total energy of manipulator system includes the kinetic energy of flexure hinges, flexible intermediate link and moving platform. The position vector relative to an inertial frame can be written as:

$$r_i = \begin{bmatrix} \cos(\alpha_i+\beta_i) & -\sin(\alpha_i+\beta_i) \\ \sin(\alpha_i+\beta_i) & \cos(\alpha_i+\beta_i) \end{bmatrix} \begin{bmatrix} (u_i(t)+x+L_{iflex}) \\ W_i(x,t) \end{bmatrix} \tag{8}$$

and derivation of Eq. (8):

$$\dot{r}_i = \begin{bmatrix} \cos(\alpha_i+\beta_i) & -\sin(\alpha_i+\beta_i) \\ \sin(\alpha_i+\beta_i) & \cos(\alpha_i+\beta_i) \end{bmatrix} \begin{bmatrix} (-W_i(x,t)\dot{\beta}_i + \dot{u}_i(t)) \\ \dot{\beta}_i(u_i(t)+x+L_{iflex}) + \dot{W}_i(x,t) \end{bmatrix} \tag{9}$$

and velocity of i^{th} intermediate flexible link is:

$$V_{ilink}^2 = \left[\dot{u}_i(t) - W_i(x,t)\dot{\beta}_i\right]^2 + \left[\dot{\beta}\left(u_i(t)+x+L_{i\,flex}\right) + \dot{W}_i(x,t)\right]^2 \tag{10}$$

which i=1, 2, 3 in above equations. The total kinetic energy of system is:

$$T = T_{flex} + T_{link} + T_P \tag{11}$$

T_P is kinetic energy of moving platform and T_{link} is kinetic energy of flexible intermediate link and T_{flex} is kinetic energy of flexure hinges. Then kinetic energy of flexible link and flexure hinges can be obtained as:

$$T_{link} = \frac{1}{2}\sum_{i=1}^{3}\int_{0}^{L_{ilink}} \rho_1[\dot{\beta}_i^2(2xL_{iflex} + u_i^2(t) + 2u_i(t)x + x^2 + L_{iflex}^2 + 2L_{iflex}u_i(t) + (W_i(x,t))^2)]dx + \frac{1}{2}\sum_{i=1}^{3}\int_{0}^{L_{ilink}} (\rho_1[\dot{\beta}_i(2u_i(t)\dot{W}_i(x,t) + 2x\dot{W}_i(x,t) - 2\dot{u}_i(t)W_i(x,t) + 2L_{iflex}\dot{W}_i(x,t)) + \dot{u}_i^2(t) + (\dot{W}_i(x,t))^2]dx \quad (12a)$$

$$T_{flex} = \frac{1}{2}\sum_{i=1}^{3}\int_{0}^{L_{flex}} \rho_0(\dot{u}_i^2(t) + \dot{\beta}_i^2(u_i(t) + L_{iflex})^2)dx \quad (12b)$$

and total kinetic energy is written as:

$$T = \frac{1}{2}\sum_{i=1}^{3}\int_{0}^{L_{flex}} \rho_0(\dot{u}_i^2(t) + \dot{\beta}_i^2(u_i(t) + L_{iflex})^2)dx + \frac{1}{2}\sum_{i=1}^{3}\int_{0}^{L_{ilink}} \rho_1[\dot{\beta}_i^2(2xL_{iflex} + u_i^2(t) + 2u_i(t)x + x^2 + L_{iflex}^2 + 2L_{iflex}u_i(t) + (W_i(x,t))^2)]dx + \frac{1}{2}\sum_{i=1}^{3}\int_{0}^{L_{ilink}} (\rho_1[\dot{\beta}_i(2u_i(t)\dot{W}_i(x,t) + 2x\dot{W}_i(x,t) - 2\dot{u}_i(t)W_i(x,t) + 2L_{iflex}\dot{W}_i(x,t)) + \dot{u}_i^2(t) + (\dot{W}_i(x,t))^2]dx + \frac{1}{2}m_p(\dot{x}_p)^2 + \frac{1}{2}m_p(\dot{y}_p)^2 + \frac{1}{2}I_p(\dot{\theta}_p)^2 \quad (12c)$$

In which ρ_0 and ρ_1 are mass per unit length of flexure hinges and mass per unit length of i^{th} link, respectively. In addition I_p is mass moment of inertia of the platform around the center point *P*, m_p is the mass of the platform, x_p and y_p are positions of platform along X-axis and Y-axis direction, respectively and θ_p is orientation of platform at the mass center *P*.

4.2 Potential energy

The potential energy was ignored due to gravitational force because it does not change during plane motion of compliant mechanism. The potential energy of intermediate link expresses the internal energy due to bending and the elastic deformation of the link. According to Euler-Bernoulli beam theory, the potential energy of the intermediate link is given as [23]:

$$V_{link} = \frac{1}{2}\sum_{i=1}^{3}\int_{0}^{L_{ilink}} E_i I_i (\frac{\partial^2 W_i(x,t)}{\partial x^2})^2 dx \quad (13)$$

where E_i is elastic modulus of the i^{th} link, and I_i is the second moment of area of the i^{th} link. In order to obtain potential energy of flexure hinges, they are modeled as revolute and prismatic joints with constant torsional and translational stiffness $k_{\theta\, flex}$ and k_{xflex}. All the first flexure hinges in each chain are assumed as a combination of torsional and translational stiffness and the second flexure hinges have just torsional stiffness. Using the formulation presented by Lobontiu, the rotational and translational stiffness of circular flexure hinge can be estimated and given as [15]:

$$\frac{1}{k_{\theta\, flex}} = \frac{\Delta\alpha}{M_z} = \frac{24R}{Ebt^3(2R+t)(4R+t)^3} \times \begin{bmatrix} t(4R+t)(6R^2+4Rt+t^2) + 6R(2R+t)^2\sqrt{t(4R+t)} \\ \arctan(\sqrt{1+\frac{4R}{t}}) \end{bmatrix} \quad (14)$$

$$\frac{1}{k_{xflex}} = \frac{\Delta x}{F_x} = \frac{1}{Eb}\left[\frac{2(2R+t)}{\sqrt{t(4R+t)}}(\tan^{-1}\sqrt{1+\frac{4R}{t}} - \frac{\pi}{2})\right] \tag{15}$$

and potential energy of flexure hinges can be estimated as:

$$V_{flex} = \frac{1}{2}k_{xflex}(u_i(t))^2 + \frac{1}{2}k_{\theta_{1i}\,flex}(\beta_i)^2 + \frac{1}{2}k_{\theta_{2i}\,flex}(\theta_p)^2 \tag{16}$$

In which $k_{\theta_1 flex}$ is torsional stiffness of first flexure hinge and $k_{\theta_2 flex}$ is torsional stiffness of second flexure hinge. The total potential energy of the system given as:

$$V = \frac{1}{2}\sum_{i=1}^{3}\int_0^{L_{ilink}} EI(\frac{\partial^2 W(x,t)}{\partial x^2})^2 dx + \frac{1}{2}k_{xflex}(u_i(t))^2 + \frac{1}{2}k_{\theta_{1i}\,flex}(\beta_i)^2 + \frac{1}{2}k_{\theta_{2i}\,flex}(\theta_p)^2 \tag{17}$$

The above assumption for flexure hinges when the first flexure hinges is designed with only 2DOF by fabricating a relatively thin neck-downed section of the flexure hinge and the second has 1DOF by fabricating a relatively thick neck-downed section.

4.3 Dynamic equations of motion using Lagrange multiplier method

The governing equations of motion are derived using Lagrange multipliers method. The Lagrangian is computed using kinetic and potential energy as follows:

$$L = T - V \tag{18}$$

The dynamic equations of compliant mechanism with flexible links, using the Lagrange multiplier method is given as [23]:

$$\frac{\partial T}{\partial \dot{q}_i} - \frac{\partial (T-V)}{\partial q_i} = Q_i + \sum_{k=1}^{6}\lambda_k \frac{\partial \eta_k}{\partial q_i} \tag{19}$$

In which Q_i is the generalized force and λ_k is k^{th} Lagrange multipliers. The method of assumed mode is applied, and flexible deformation of the i^{th} intermediate link can be expressed as:

$$W_i(x,t) = \sum_{j=1}^{r}\delta_{ij}(t)\varphi_{ij}(x) \tag{20}$$

Functions $\delta_{ij}(t)$ can be considered as generalized coordinates expressing the deformation of the linkage and functions $\varphi_{ij}(x)$ are referred to as assumed modes. The clamped-clamped boundary condition is assumed for the intermediate links. The eigen function of clamped-clamped beam was derived based on Euler-Bernoulli beam theory. According to Euler-Bernoulli beam theory, position-dependent mode shape function for clamped-clamped beam is selected as [19]:

$$\varphi_j(x) = \cosh(\frac{\eta_j x}{l}) - \cos(\frac{\eta_j x}{l}) - \sigma_j(\sinh(\frac{\eta_j x}{l}) - \sin(\frac{\eta_j x}{l})) \tag{21}$$

and σ_j are [19]:

$$\sigma_j = \frac{\cosh(\eta_j) - \cos(\eta_j)}{\sinh(\eta_j) - \sin(\eta_j)} \tag{22}$$

In which η_j is the root of the characteristic or frequency equation, and frequency equation of clamped-clamped beam is given as [19]:

$$\cos(\eta_j)\cosh(\eta_j) = 1 \tag{23}$$

Generalized coordinates for the compliant mechanism with flexible links are β_i , u_i ,δ_{ij} , x_p ,y_p ,θ_p . The number of generalized coordinates is $9+3r$, $r=1,2,3$. For the present compliant mechanism the number of degrees of freedom is $3+3r$. Therefore the number of generalized coordinate is greater than the number of degree of freedom of compliant mechanism. Then six constraint equations should be considered in equations of motion. The constraint equations obtained from closed-loop chains as shown in Fig. 3:

$$\overline{A_1A_i} + \overline{A_iB_i} + \overline{u_i} + \overline{L_i} + \overline{C_iP} = \overline{A_1P} \ , \quad i=1,2,3 \tag{24}$$

Equivalence of the real and imaginary parts of both sides of above relation leads to:

$$\begin{aligned}
&\eta_{2i-1} = u_i\cos(\alpha_i+\beta_i(t)) + (l_{flex}+l)\cos(\alpha_i+\beta_i(t)) - x_p - \tilde{l}_p\cos(\theta_p) = 0\\
&\eta_{2i} = u_i\sin(\alpha_i+\beta_i(t)) + (l_{flex}+l)\sin(\alpha_i+\beta_i(t)) - y_p - \tilde{l}_P\sin(\theta_p) = 0
\end{aligned} \tag{25}$$

Eqs. (25) are six constraint equations. Substituting Eqs. (12), (17) and (20) into (18) and (19), and Eq.(19) is formulated as follows:

$$\begin{aligned}
&\frac{\partial T}{\partial \dot{u}_i} - \frac{\partial (T-V)}{\partial u_i} = \rho_0 A_0 \ddot{u}_i(t) + m_1\ddot{u}\ (t) - 2Q_2\dot{\delta}_{ij}\dot{\beta}_i(t)\\
&-Q_2\delta_{ij}\dot{\beta}_i^2(t) + \rho_0 A_0(l_{flex}+u_i(t))\dot{\beta}_i^2(t) - m_1 u_i(t)\dot{\beta}_i^2(t) -\\
&\frac{m_1 l}{2}\dot{\beta}_i^2(t) - m_1 l_{flex}\dot{\beta}_i^2(t) + k_{xi}u_i(t) =\\
&\lambda_{2i-1}\cos(\alpha_i+\beta_i(t)) + \lambda_{2i}\sin(\alpha_i+\beta_i(t))
\end{aligned} \tag{26}$$

$$\begin{aligned}
&\frac{\partial T}{\partial \dot{\beta}_i} - \frac{\partial (T-V)}{\partial \beta_i} = 2\rho_0 A_0(l_{flex}+u_i(t))\dot{\beta}_i\dot{u}_i + \rho_0 A_0(l_{flex}+u_i(t))^2\ddot{\beta}_i(t) + m_1(l_{flex}\ddot{\beta}_i(t) +\\
&u_i(t)\dot{\beta}_i\dot{u}_i(t) + u_i^2(t)\ddot{\beta}_i + l\dot{u}_i(t)\dot{\beta}_i(t) + u_i(t)l\ddot{\beta}_i(t) + \frac{l^2}{3}\ddot{\beta}_i(t) + l_{flex}^2\ddot{\beta}_i(t) + 2l_{flex}\dot{u}_i(t)\dot{\beta}_i(t) +\\
&2l_{flex}u_i(t)\ddot{\beta}_i(t)) + u_i(t)Q_{ij}^2\ddot{\delta}_{ij}(t) + Q_{ij}^3\ddot{\delta}_{ij}(t) - \ddot{u}_i(t)Q_{ij}^2\delta_{ij}(t) + l_{flex}Q_{ij}^2\ddot{\delta}_{ij}(t) + 2Q_{ij}^1\delta_{ij}(t)\dot{\beta}_i(t)\dot{\delta}_{ij}(t) +\\
&Q_{ij}^1\delta_{ij}^2(t)\ddot{\beta}_i(t) + k_\theta\beta_i(t) = M_{ia} - \lambda_{2i-1}(u_1+l_{flex}+l)\sin(\alpha_i+\beta_i(t)) + \lambda_{2i}(u_1+l_{flex}+l)\cos(\alpha_i+\beta_i(t))
\end{aligned} \tag{27}$$

$$\frac{\partial T}{\partial \dot{\delta}_{ij}} - \frac{\partial (T-V)}{\partial \delta_{ij}} = Q_{ij}^1\ddot{\delta}_{ij}(t) + 2\dot{u}_i\dot{\beta}_i Q_{ij}^2 + u_i Q_{ij}^2\ddot{\beta}_i + Q_{ij}^3\ddot{\beta}_i + l_{iflex}Q_{ij}^2\ddot{\beta}_i - Q_{ij}^1\delta_{ij}(t)(\dot{\beta}_i)^2 + EI\delta_{ij}Q_{ij}^4 = 0 \tag{28}$$

$$\frac{\partial T}{\partial \dot{y}_p} - \frac{\partial (T-V)}{\partial y_p} = m_p\ddot{y}_p = -\lambda_2 - \lambda_4 - \lambda_6 \tag{29}$$

$$\frac{\partial T}{\partial \dot{x}_p} - \frac{\partial (T-V)}{\partial x_p} = m_p\ddot{x}_p = -\lambda_1 - \lambda_3 - \lambda_5 \tag{30}$$

In which:

$$Q_{ij}^{1}=\int_{0}^{L_{ilink}}\rho_1(\varphi_{ij}(x))^2\,dx \quad , \quad Q_{ij}^{2}=\int_{0}^{L_{ilink}}\rho_1(\varphi_{ij}(x))dx$$
$$Q_{ij}^{4}=\int_{0}^{L_{ilink}}(\varphi_{ij}''(x))^2\,dx \quad , \quad Q_{ij}^{3}=\int_{0}^{L_{ilink}}\rho_1(\varphi_{ij}(x))x\,dx \tag{31}$$

Eq. (28) can be rewritten in matrix form as:

$$M\ddot{\delta}+K\delta+P\ddot{\beta}=F_{cor} \tag{32}$$

where M is the modal mass matrix, K is the modal stiffness matrix, $P\ddot{\beta}$ is the effect of rigid-body motion on elastic vibration of flexible links, F_{cor} is Coriolis force.

4.4 Dynamic equations of motion using Kane's method

In this section, the Kane's Method is employed to derive the governing equation of motion for the compliant mechanism with flexible links. We select the generalized speed as:

$$u_1=\dot{u}(t) \quad , \quad u_2=\dot{\beta}(t) \quad , \quad u_3=\dot{\delta}(t) \quad , \quad u_4=\dot{X}_P \quad , \quad u_5=\dot{Y}_P \quad , \quad u_6=\dot{\theta}_P \tag{33}$$

The velocity of point G for flexible links can be obtained as follow:

$$V_G=[(-W_i(x,t)\dot{\beta}_i+\dot{u}_i(t))\cos(\alpha_i+\beta_i)+(\dot{\beta}_i(u_i(t)+x+L_{iflex})+\dot{W}_i(x,t))(-\sin(\alpha_i+\beta_i))]i+$$
$$[(-W_i(x,t)\dot{\beta}_i+\dot{u}_i(t))\sin(\alpha_i+\beta_i)+(\dot{\beta}_i(u_i(t)+x+L_{iflex})+\dot{W}_i(x,t))(\cos(\alpha_i+\beta_i))]j \tag{34}$$

and the acceleration of point G for intermediate flexible links can be obtained as below:

$$a_G=[(-\dot{W}_i(x,t)\dot{\beta}_i-W_i(x,t)\ddot{\beta}+\ddot{u}_i(t))\cos(\alpha_i+\beta_i)-\dot{\beta}_i(-W_i(x,t)\dot{\beta}_i+\dot{u}_i(t))\sin(\alpha_i+\beta_i)-$$
$$(\ddot{\beta}_i(u_i(t)+x+L_{iflex})+\ddot{W}_i(x,t)+\dot{\beta}_i\dot{u}_i(t))(\sin(\alpha_i+\beta_i))-(\dot{\beta}_i^2(u_i(t)+x+L_{iflex})+$$
$$\dot{\beta}_i\dot{W}_i(x,t))(\cos(\alpha_i+\beta_i))]i+[(-\dot{W}_i(x,t)\dot{\beta}_i-W_i(x,t)\ddot{\beta}+\ddot{u}_i(t))\sin(\alpha_i+\beta_i)+ \tag{35}$$
$$\dot{\beta}_i(-W_i(x,t)\dot{\beta}_i+\dot{u}_i(t))\cos(\alpha_i+\beta_i)+(\ddot{\beta}_i(u_i(t)+x+L_{iflex})+\ddot{W}_i(x,t)+$$
$$\dot{\beta}_i\dot{u}_i(t))(\cos(\alpha_i+\beta_i))-(\dot{\beta}_i^2(u_i(t)+x+L_{iflex})+\dot{\beta}_i\dot{W}_i(x,t))(\sin(\alpha_i+\beta_i))]j$$

To obtain dynamic equation of motion for flexible generalized coordinate, partial velocity respect to $u_3=\dot{\delta}(t)$ can be obtain as following equation:

$$V_G^k=\frac{\partial V_G}{\partial u_3}=-\varphi_{ij}(x)\sin(\alpha_i+\beta_i)i+\varphi_{ij}(x)\cos(\alpha_i+\beta_i)j \tag{36}$$

The generalized inertia forces of the flexible links can be obtained from the below equation:

$$U_k^*=-\int_{0}^{l_{link}}ma_{Gi}\cdot V_{Gi}^k dx=-\int_{0}^{l_{link}}\rho[\dot{\beta}_i(-W_i(x,t)\varphi_{ij}(x)\dot{\beta}_i+\varphi_{ij}(x)\dot{u}(t))+$$
$$(\ddot{\beta}_i(\varphi_{ij}(x)u_i(t)+\varphi_{ij}(x)x+\varphi_{ij}(x)l_{flex})+\varphi_{ij}(x)\dot{\beta}_i\dot{u}_i(t)+\varphi_{ij}(x)\ddot{W}_i(x,t)]dx \tag{37}$$

Substituting Eq. (20) into Eq. (37) generalized inertia force can be obtained as follow:

$$U_k^* = -\int_0^{l_{link}} ma_{Gi} \cdot V_{Gi}^k dx = -\int_0^{l_{link}} \rho[\dot{\beta}_i(-\sum_{j=1}^{r} \delta_{ij}(t)\varphi_{ij}^2(x)\dot{\beta}_i + \varphi_{ij}(x)\dot{u}(t)) + (\ddot{\beta}_i\varphi_{ij}(x)(u_i(t)+x+l_{flex}) + \dot{\beta}_i\dot{u}_i(t)\varphi_{ij}(x) + \sum_{j=1}^{r} \ddot{\delta}_{ij}(t)\varphi_{ij}^2(x)]dx \quad (38)$$

or

$$U_k^* == -(-Q_{ij}^{1*}\dot{\beta}_i^2\delta_{ij}(t) + Q_{ij}^{1*}\ddot{\delta}_{ij}(t) + \int_0^{l_{link}} \{2\varphi_{ij}(x)\dot{\beta}\dot{u}(t) + \ddot{\beta}_i\varphi_{ij}(x)(u_i(t)+x+l_{flex})\}dx) \quad (39)$$

In which:

$$Q_{ij}^{1*} = \int_0^{l_{link}} \rho\varphi_{ij}^2(x)dx \quad , \quad Q_{ij}^{2*} = \int_0^{l_{link}} (\varphi''(x))^2 dx \quad (40)$$

and now the generalized active forces of the flexible link can be obtained as below:

$$U_k = -\frac{\partial V_{link}}{\partial q_k} = \frac{\partial V_{link}}{\partial \delta_{ij}(t)} = E_i I_i \delta_{ij}(t) Q_{ij}^{2*} \quad (41)$$

According to the Kane's method the generalized inertia forces and the generalized active forces constitute the equations of motion as below [23]:

$$U_k + U_k^* = 0 \quad (42)$$

Substituting Eq. (39) and Eq. (41) into Eq. (42), and the equation of motion can be obtained as follow:

$$(-Q_{ij}^{1*}\dot{\beta}_i^2\delta_{ij}(t) + Q_{ij}^{1*}\ddot{\delta}_{ij}(t) + \int_0^{l_{link}} \{2\varphi_{ij}(x)\dot{\beta}\dot{u}(t) + \ddot{\beta}_i\varphi_{ij}(x)(u_i(t)+x+l_{flex})\}dx) + E_i I_i \delta_{ij}(t) Q_{ij}^{2*} = 0 \quad (43)$$

and finally the equations of motion for flexible link of compliant mechanism can be obtained from following equation:

$$-Q_{ij}^{1*}\dot{\beta}_i^2\delta_{ij}(t) + Q_{ij}^{1*}\ddot{\delta}_{ij}(t) + 2Q_{ij}^2\dot{\beta}\dot{u}(t) + Q_{ij}^2\ddot{\beta}_i u_i(t) + Q_{ij}^2\ddot{\beta}_i l_{flex} + Q_3^*\ddot{\beta} + E_i I_i \delta_{ij}(t) Q_{ij}^{2*} = 0 \quad (44)$$

The comparison of the Eq. (44) and Eq. (28) shows that the Lagrange and Kane's Methods yielded similar results. In addition, these results verify the equations of motion which is obtained by Lagrange Method. For getting frequency equation, we use equations of motion in Eq. (28) and for considering a constant angular velocity of intermediate link and assuming time-independent axial displacement, one gets:

$$-Q_{ij}^1(\omega^2) - Q_{ij}^1(\dot{\beta}_i)^2 + EIQ_{ij}^4 = 0 \quad (45)$$

In the above equation $\frac{\ddot{\delta}(t)}{\delta(t)} = -(\omega^2)$, the equivalent frequency may be evaluated by:

$$(\omega^2) = \frac{-Q_{ij}^1(\dot{\beta}_i)^2 + EIQ_{ij}^4}{Q_{ij}^1} \quad (46)$$

Consequently, from Eq. (46), the natural frequency for the link decreases with angular velocity and for the clamped-clamped boundary condition we have:

$$Q_{ij}^{4} = (\frac{(1+j)\pi}{l})^{4} Q_{ij}^{41} \tag{47}$$

By substituting Eq. (48) into Eq. (47), frequency can be obtained as:

$$(\omega^{2}) = \frac{EI((1+j)\pi)^{4}}{l^{4} Q_{ij}^{1}} Q_{ij}^{41} - (\dot{\beta}_{i})^{2} \tag{48}$$

Therefore, the first term on the right side of the Eq. (48) is the natural frequency expression for non-rotating beam. Eq. (48) is similar to the one result given in ref. [14].

5 SOLUTION METHODOLOGY

To solve equations of motion the perturbation method is used, which consists of determining the series convergent to the exact solution. Using Taylor series to expand the terms in Eq. (28) or (44), we have:

$$Q_{ij}^{1} \frac{d^{2}\delta_{ij}(t)}{dt^{2}} + (a_{1}Q_{ij}^{2} - a_{2}Q_{ij}^{3} + a_{3}Q_{ij}^{2}t - a_{4}Q_{ij}^{2}t^{2})\delta_{ij}(t) - a_{5}Q_{ij}^{1} + a_{6}Q_{ij}^{4} - a_{7}Q_{ij}^{1}t - a_{8}Q_{ij}^{1}t^{2} = 0 \tag{49}$$

For mode1, we have:

$$Q_{11}^{1} \frac{d^{2}\delta(t)}{dt^{2}} + (b_{1} + \varepsilon)\delta(t) - a_{5}Q_{11}^{1} + a_{6}Q_{11}^{4} - a_{7}Q_{11}^{1}t - a_{8}Q_{11}^{1}t^{2} = 0 \tag{50}$$

when ε is small but is different from zero and $b_1 >> \varepsilon$, we suppose that the solution of above equation can be expressed in the form [25]:

$$\delta(t,\varepsilon) = \delta_{0}(t) + \varepsilon\delta_{1}(t) + \varepsilon^{2}\delta_{2}(t) + \ldots \tag{51}$$

Substitute Eq. (51) into Eq. (50) and set ε=0 and obtained:

$$Q_{11}^{1}\ddot{\delta}_{0} + (b_{1})\delta_{0}(t) - a_{5}Q_{11}^{1} + a_{6}Q_{11}^{4} - a_{7}Q_{11}^{1}t - a_{8}Q_{11}^{1}t^{2} = 0 \tag{52}$$

$$Q_{11}^{1}\ddot{\delta}_{1} + (b_{1})\delta_{1}(t) + \delta_{0}(t) = 0 \tag{53}$$

The general solution of Eq. (52) can be written as:

$$\delta_{0}(t) = A_{0}\cos(t + \beta_{0}) + f(t) \tag{54}$$

where A_0, β_0 are arbitrary constant. Therefore Eq. (53) can be re-written as:

$$Q_{11}^{1}\ddot{\delta}_{1} + (b_{1})\delta_{1}(t) + A_{0}\cos(t + \beta_{0}) + f(t) = 0 \tag{55}$$

The homogeneous and particular solutions are:

$$\delta(t) = A_{0}\cos(t + \beta_{0}) + f(t) + \varepsilon(A_{1}\cos(t + \beta_{1}) + f_{1}(t)) + \ldots \tag{56}$$

and flexible deformation of the first intermediate link for mode 1 can be expressed as:

$$W_1(x,t) = \delta\ (t)\varphi_1(x) \tag{57}$$

6 NUMERICAL RESULTS AND DISCUSSION

In the present compliant mechanism, dynamic analysis of parallel compliant mechanism with flexible links and rigid moving platform is considered. Geometrical and material properties of flexible link are given in Table 1. The geometrical properties for flexure hinges are given in Table 3. Flexures and intermediate links are modeled as aluminum alloy.

The number of degree of freedom (DOF) for present compliant mechanism is $3+3r$, in which 3 degrees of rigid body degree and $3r$ degrees of elastic motion. Dynamic equation is including of $9+3r$ differential equations and 6 constraint equations. All three joints are controlled separately using proportional and derivative (PD) feedback control with gains k_p and k_d. Thus the deriving moments applied to three flexure hinges are given as:

$$M_{ia} = k_p(\beta_{di} - \beta_i) + k_d(\dot{\beta}_{di} - \dot{\beta}_i) \tag{58}$$

β_{di} are desired angle of flexure hinge. The deflection of flexure hinges and intermediate links is determined based on the prescribed motion of the moving platform. To obtain the deflection, velocity, angular velocity, and acceleration, inverse kinematics was used. From inverse kinematics, the displacement and velocity of flexure hinges are given as:

$$\begin{aligned} u_i^2 = {} & (X_P - (l_{i.\,flex} + L_i)\cos(\alpha_i + \beta_i) - C_iG\cos(\alpha_{C_iG} + \theta) - A_1A_i\cos(\alpha_{A_1A_i}))^2 + \\ & (Y_P - (l_{i.\,flex} + L_i)\sin(\alpha_i + \beta_i) - C_iG\sin(\alpha_{C_iG} + \theta) - A_1A_i\sin(\alpha_{A_1A_i}))^2 \end{aligned} \tag{59}$$

$$\dot{u}_i = \cos(\alpha_i + \beta_i(t))\dot{x}_p + \sin(\alpha_i + \beta_i(t))\dot{y}_p \tag{60}$$

Angular velocities of intermediate links are given as:

$$\dot{\beta}_i = \frac{1}{-(u_i + L_i + l_{iflex})}(-\sin(\alpha_i + \beta_i(t))\dot{x}_p + \cos(\alpha_i + \beta_i(t))\dot{y}_p) \tag{61}$$

Micro-motion system consists of 3 Tokin AE1515D16 [9], PZT stack actuators assembled into flexure hinges of compliant mechanism. According to Eqs. (3-4-5-6-7), the axial displacement of flexure hinges is obtained and comparison u with last work by Paros and Weisbord and Lobontiu are given in Table 2. and illustrated in Fig. 5.

Table 1
Compliant mechanism physical parameters

$L_1 = L_2 = L_3\ (m)$	α_1(deg)	α_2(deg)	α_3(deg)	$A(m^2)$	$I\ (m^4)$	$\rho\ (kg/m^3)$	E (N/m^2)
0.05249	38	158	278	0.18e-4	1.35e-11	2.77e3	7.1e10

Table 2
Comparisons of various compliance equations with this study

Case	u	error
Paros and Weisbord	0.5676e-3(m)	3.6%
Lobontiu	0.5446e-3(m)	8.6%
This study	0.5885e-3(m)	-

Table 3
Geometrical properties of flexure hinge

L_{iflex}	B	t	R	d
0.006(m)	3(mm)	0.5(mm)	3(mm)	9(mm)

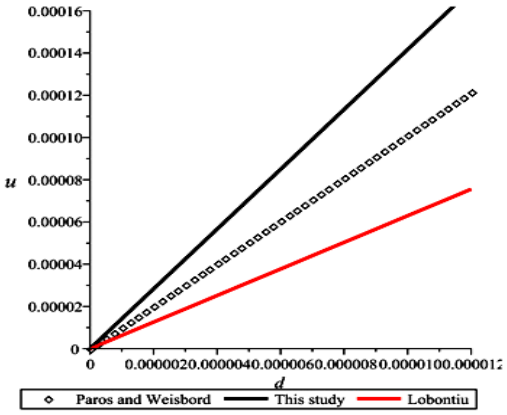

Fig. 5
Variation of axial displacement of flexure hinges vs. variation of PZT actuator.

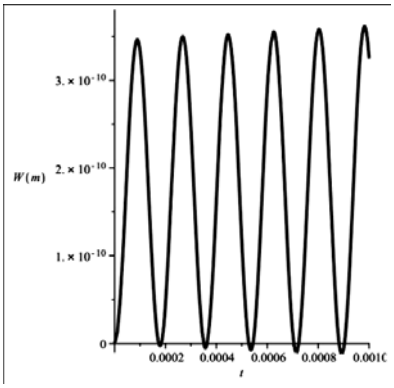

(a)

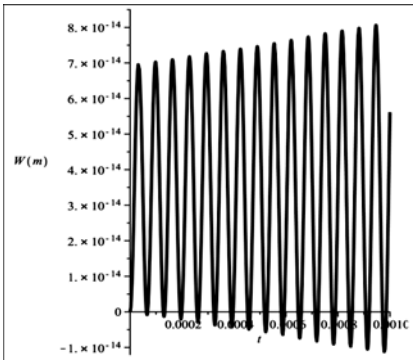

(b)

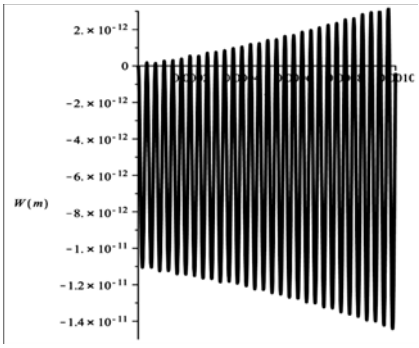

(c)

Fig. 6
First three vibration modes of the 1st intermediate link at the midpoint (a): Mode 1, (b): Mode 2, (c): Mode 3.

In this simulation, the moving platform is set to move on a desired trajectory given as:

$$x_p = C_1 + \frac{x_f}{t_f}t - \frac{x_f}{2\pi}\sin(\frac{2\pi}{t_f}t)$$
$$y_p = C_2 + \frac{x_f}{t_f}t - \frac{x_f}{2\pi}\sin(\frac{2\pi}{t_f}t) \quad (62)$$
$$\theta = const$$

where $x_f = 0.2mm$ and $t_f = 1ms$ and $C_1 = 0.039, C_2 = 0.041$. And flexible generalized coordinate in the Eq. (25) are: $\delta_{ij} = [\delta_{11}\ \delta_{12}\ \delta_{13}\ \delta_{21}\ \delta_{22}\ \delta_{23}\ \delta_{31}\ \delta_{32}\ \delta_{33}]$. To solve Eq. (28), initial conditions are adopted $\delta_{ij} = 0$, $\dot{\delta}_{ij} = 0$ .The deflection of the midpoint of the intermediate links for 3modes is obtained using perturbation method and Runge-Kutta-Fehlberg 4, 5th. Fig. 6 shows the amplitude of the first three mode vibration of the first intermediate flexible link at the midpoint and reveals that the amplitude of the first mode vibration is larger than the amplitude of the second mode vibration and first mode is sufficiently accurate to describe the vibration of flexible link.

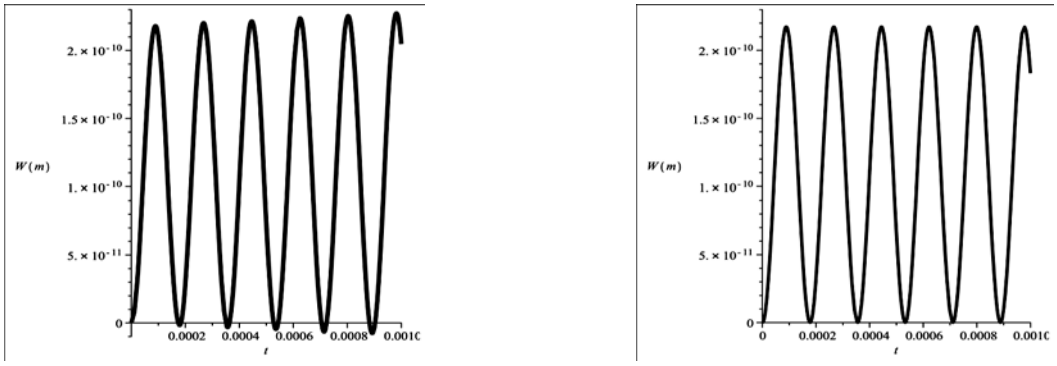

(a) (b)

Fig. 7
The compared results between Perturbation method with Runge-Kutta-Fehlberg 4,5th order for mode1. (a): RKF 4,5th (b): perturbation method.

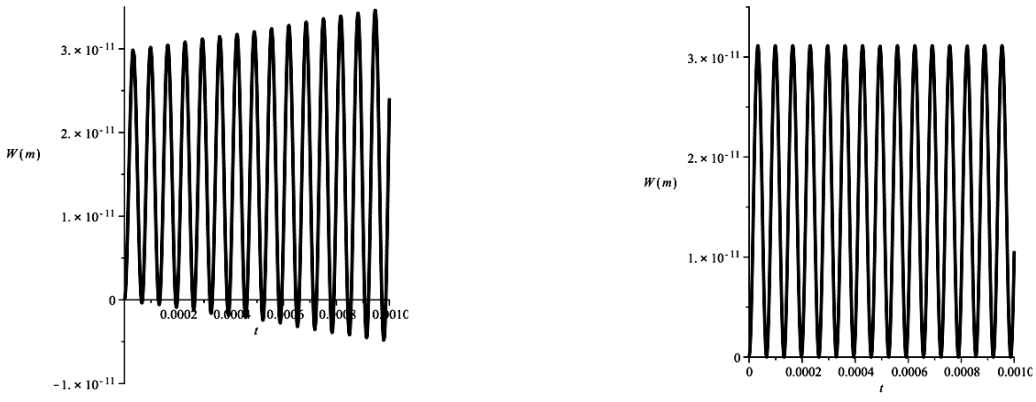

(a) (b)

Fig. 8
The compared results between Perturbation method with Runge-Kutta-Fehlberg 4,5th order for mode2. (a): RKF 4,5th (b): perturbation method.

The comparison of the deflection versus time for results obtained from perturbation method and Runge-Kutta-Fehlberg 4,5th order has been depicted in Fig. 7and Fig. 8.

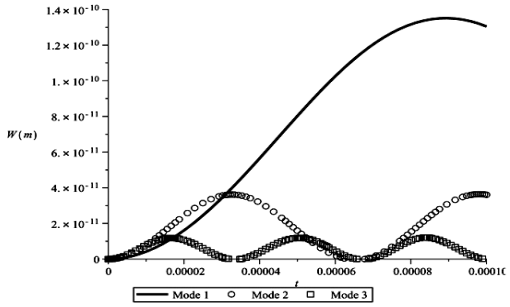

Fig. 9
First three vibration modes of the 1st intermediate link at the x=L/5.

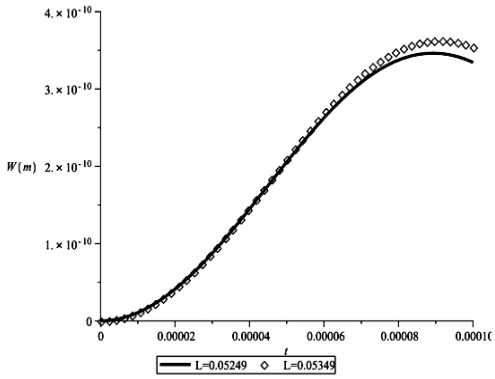

Fig. 10
The effect of intermediate link length on deflection.

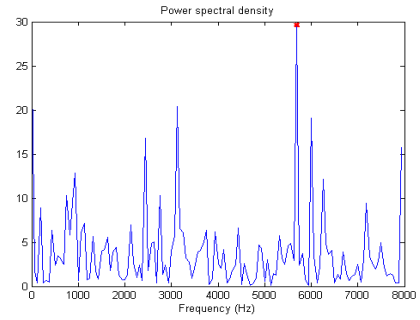

(a)

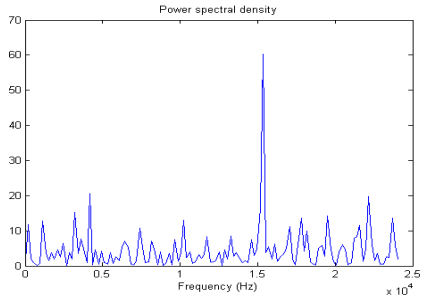

(b)

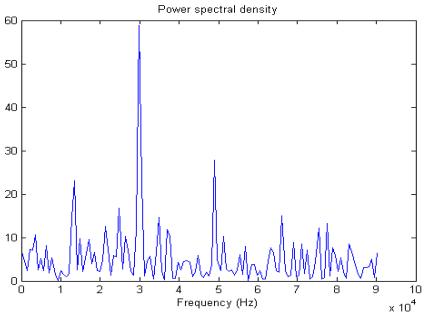

(c)

Fig. 11
Frequency spectra of vibration for the 1st link (a): Mode 1, (b): Mode 2, (c): Mode 3.

It can be observed that there is an excellent agreement between the results obtained from perturbation method with those of Runge-Kutta-fehlberg 4,5th order method. Fig. 9, shows the amplitude of the first three modes vibration of the first intermediate link at x=L/5. The effect of hinge length on deflection of midpoint of first link is illustrated in Fig. 13. It shows that when hinge length increases, the deflection of midpoint of link increases. The selected lengths of hinges for this simulation are $l_{flex} = 0.00625(m)$, $l_{flex} = 0.00725(m)$.

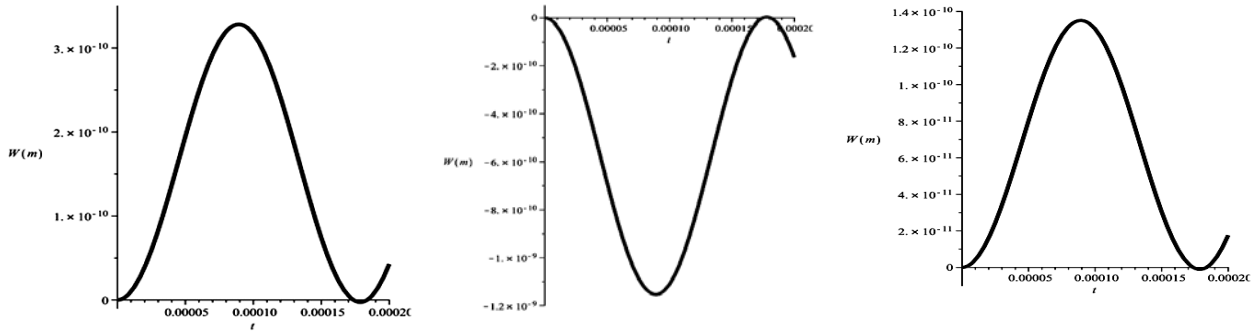

(a) (b) (c)

Fig. 12
Deflection at the midpoint of intermediate links (a): link 1, (b): link2, (c): link3.

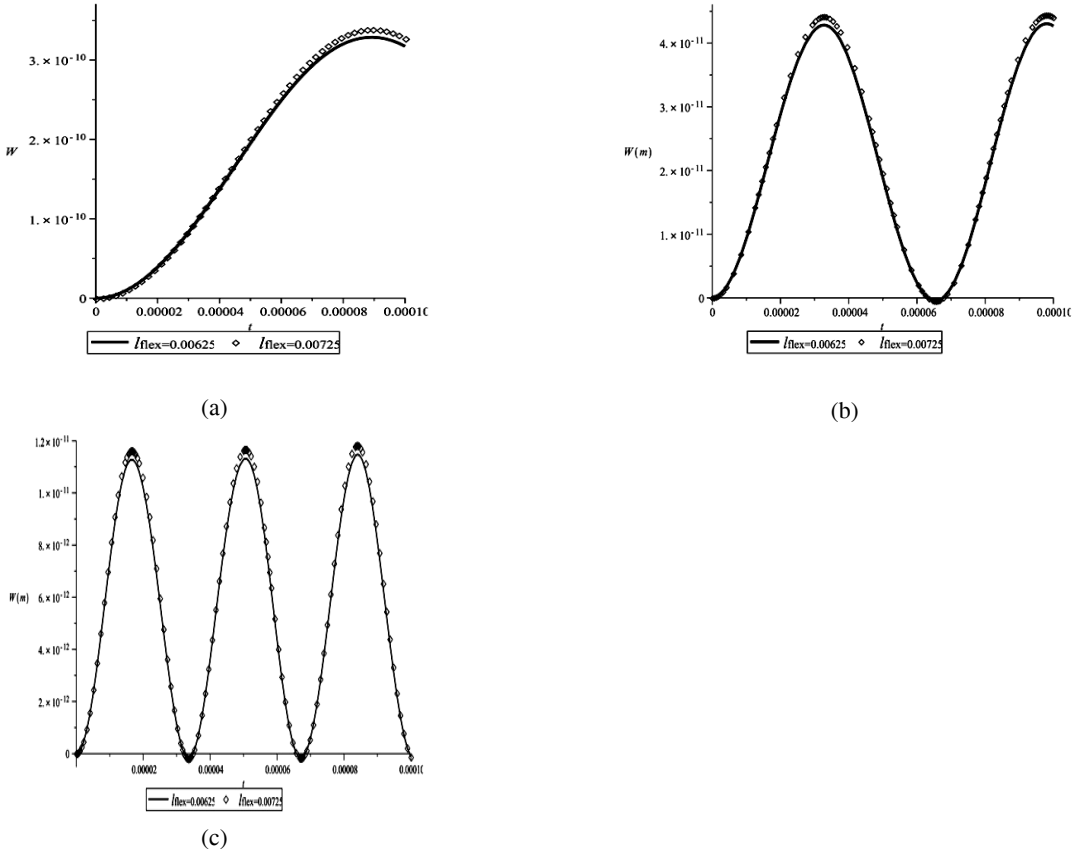

(a) (b)

(c)

Fig. 13
The effect of flexure hinge length on deflection of midpoint of first intermediate link for fist three modes. (a):Mode 1, (b): Mode 2, (c): Mode 3 .

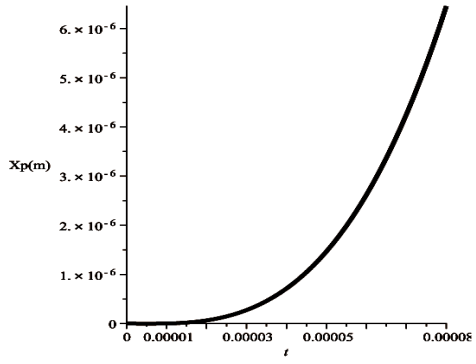

Fig. 14
Position of the platform along X axis.

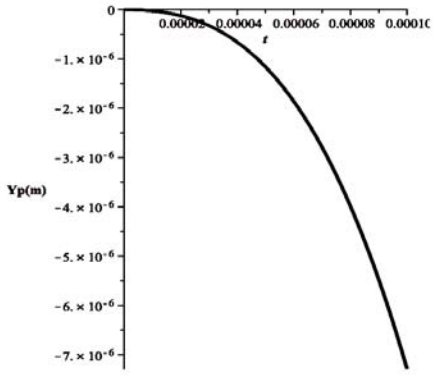

Fig. 15
Position of the platform along Y axis.

It reveals that amplitude of the first mode of vibration is larger than the amplitude of the second and third mode of vibration. In Fig. 10 effect of intermediate link length on deflection is illustrated. By increasing intermediate link size, deflection of midpoint increase. The corresponding frequency spectra analysis is performed using the Fast Fourier Transform (FFT).The power density of frequency spectra for vibration response of the first intermediate link at midpoint is shown in Fig.11. According to the Eq. (25), first three mode frequencies calculated to be 5629.67, 15493.65, 30423.10. These are the frequencies of the FFT analysis. Fig. 12 shows the elastic vibration at the midpoint of intermediate links. The vibration amplitudes for each links are different from each other due to their different base motions. According to Lagrange multipliers method, the displacement of the moving platform along *X* and *Y* axes, calculated based on Eqs. (26, 27, 28, 29, 30), are given in Fig. 14 and Fig. 15.

7 CONCLUSION

In this paper, the kinematic and dynamic modeling of a compliant parallel micro-positioning mechanism with flexible links is considered. The dynamic equations are derived using Lagrange multiplier and Kane's methods. Perturbation and RKF methods are adopted for the solution of dynamic equation of motion and the mode shape functions are selected by modeling intermediate link as Euller-Bernouli beam theory with clamped-clamped boundary conditions. The corresponding frequency spectra analysis is performed using the FFT. Based on numerical results, it is concluded that:

- Comparing Kane's method and Lagrange method leads to same results but Kan's method is faster than Lagrange method to obtaining dynamic equations.
- For three intermediate links, the elastic deflections are different due to their different base motions.
- There is an excellent agreement between the results obtained from perturbation method with those of Runge-Kutta-Fehlberg 4,5th order method.
- Increasing of the flexure hinge's length causes the deflection of intermediate links at certain time to increase.

- Natural frequencies of three first modes were obtained by using the FFT spectral.
- Using Lagrange multiplier method, the position of the moving platform can be obtained.

REFERENCES

[1] Lobontiu N., 2003, *Compliant Mechanisms Design of Flexure Hinges*, CRC Press, Florida.

[2] Yi B.J., Chung G.B., Na H.Y., Kim W.K., Suh I.H., 2003, Design and experiment of a 3-DOF parallel micromechanism utilizing flexure hinges, *IEEE Transactions on Robotics and Automation* **19**: 604-612.

[3] Yong Y.K., Fu L.T., 2009, Kinetostatic modeling of a 3-RRR compliant micro-motion stages with flexure hinges, *Mechanism and Machine Theory* **44**: 1156-1175.

[4] Yong Y.K., Fu L.T., 2008, The effect of the accuracies of flexure hinge equations on the output compliances of planar micro-motion stages, *Mechanism and Machine Theory* **43**: 347-363.

[5] Yong Y.K., Fu L.T., 2009, Comparison of circular flexure hinge design equations and the derivation of empirical stiffness formulations, *IEEE/ASME International Conference on Advanced Intelligent Mechatronics Suntec Convention and Exhibition Center*, doi:10.1109/AIM.2009.5229961.

[6] Paros J.M., Weisbord L., 1965, How to design flexure hinges, *Machine Design* **37**: 151-156.

[7] Anathasuresh G.K., Kota S., 1995, Designing compliant mechanisms, *ASME Mechanical Engineering* **117**: 93-96.

[8] Murphy M.D., Midha A., Howell L.L., 1996, The topological synthesis of compliant mechanisms, *Mechanism and Machine Theory* **31**: 185-199.

[9] Tokin, 1996, *Multilayer Piezoelectric Actuators*, User's Manual, Tokin Corporate Publisher.

[10] Saggere L., Kota S., 1997, Synthesis of distributed compliant mechanisms for adaptive structures application: an elasto-kinematic approach, *Proceedings of the DETC 1997, ASME Design Engineering Technical Conferences, Sacramento, CA*.

[11] Kota S., Joo J., Li Z., Rodgers S.M., Sniegowski J., 2001, Design of compliant mechanisms: applications to MEMS, *Analog Integrated Circuits and Signal Processing-An international journal* **29**: 7-15.

[12] Rong Y.,Zhu Y., Luo Z., Xiangxi L., 1994, Design and analysis of flexure hinge mechanism used in micro-positioning stages, *ASME proceeding of the 1994 international Mechanical Engineering Congress and Exposition* **68**: 979-985.

[13] Her I., Cheng J.C., 1994, A linear scheme for the displacement analysis of micro positioning stages with flexure hinges, *ASME Journal of Mechanical Design* **116**: 770-776.

[14] Trindade M.A., Sampaio R., 2002, Dynamics of beams undergoing large rotations accounting for arbitrary axial deformation, *AIAA journal of Guidance, Control and dynamics* **25**: 634-643.

[15] Yong Y.K., Lu T.F., Handley D.C., 2008, Review of circular flexure hinge design equations and derivation of empirical formulations, *Precision Engineering* **32**: 63–70.

[16] Lobontiu N., Paine J.S.N., Garcia E., Goldfarb M., 2001, Corner-filleted flexure hinges, *Transactions of the ASME, Journal of Mechanical Design* **123**: 346-352.

[17] Shim J., Song S.K., Kwon D.S., Cho H.S., 1997, Kinematic feature analysis of a 6-degree of freedom in-parallel manipulator for micro-positioning surgical, *Proceedings of 1997 IEEE/RSJ International Conference on Intelligent Robots and Systems* **3**:1617-1623.

[18] Ryu J.W., Gweon D., Moon K.S., 1997, Optimal design of a flexure hinge based xyθ wafer stage, *Precision Engineering* **21**: 18-28.

[19] Meirovitch L., 2001, *Fundamentals of Vibrations*, MC Grow Hill, New York.

[20] Yu H.Y., Bi S., Zong G., Zhao W., 2004, Kinematics feature analysis of a 3 DOF compliant mechanism for micro manipulation, *Chinese Journal of Mechanical Engineering* **17**: 127-131.

[21] Choi K.B., Kim D.H., 2006, Monolithic parallel linear compliant mechanism for two axes ultraprecision linear motion, *Review of Scientific Instruments* **77**(6): 065106.

[22] Tian Y., Shirinzadeh B., Zhang D., Zhong Y., 2010, Three flexure hinges for compliant mechanism designs based on dimensionless graph analysis, *Precision Engineering* **34**: 92–100.

[23] Baruh H., 1999, *Analytical Dynamics*, McGraw-Hill.

[24] Dwivedy S.K., Wberhard P., 2006, Dynamic analysis of flexible manipulators, a literature review, *Mechanism and Machine Theory* **41**: 749-777.

[25] Nayfeh A.H., 1981, *Introduction to Perturbation Techniques*, John Wiley & Sons, Inc.

[26] Benosman M., Vey G.L., 2004, Control of flexible manipulators: a survey, *Robotica* **22**: 533-545.

[27] Lee J.D., Geng Z., 1993, Dynamic model of a flexible Stewart platform, *Computers and Structures* **48**: 367-374.

[28] Zhou Z., Xi J., Mechefske C.K., 2006, Modeling of a fully flexible 3PRS manipulator for vibration analysis, *Journal of Mechanical Design* **128**: 403-412.

[29] Piras G., Cleghorn W.L., Mills J.K., 2005, Dynamic finite-element analysis of planar high speed, high-precision parallel manipulator with flexible links, *Mechanism and Machine Theory* **40**: 849-862.

[30] Wang X., Mills J.K., 2005, FEM dynamic model for active vibration control of flexible linkages and its application to a planar parallel manipulator, *Journal of Applied Acoustics* **66**: 1151-1161.